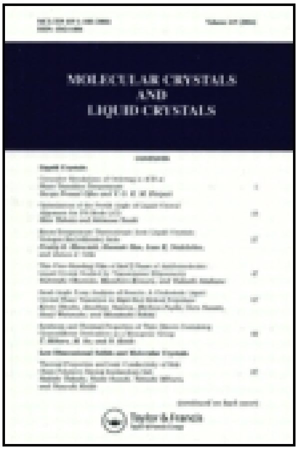

Molecular Crystals and Liquid Crystals
Publication details, including instructions for authors and subscription information:
http://www.tandfonline.com/loi/gmcl16

Grain Boundaries Obsevation of Polycrystalline Sillcon Using Nematic Liquid Crystals with Positive Dielectric Anisotropy

Toshio Takeuchi [a], Tadashi Takahashi [a] & Tatsuo Uchida [b]
[a] Department of Electronic Engieering, Sendai Radio Technical College, Miyagicho, Miyagi, 989-31, Japan
[b] Department of Electronic Engineering, Faculty of Engineering, Tohoku University, Sendai, 980, Japan

Version of record first published: 17 Oct 2011.

To cite this article: Toshio Takeuchi , Tadashi Takahashi & Tatsuo Uchida (1985): Grain Boundaries Obsevation of Polycrystalline Sillcon Using Nematic Liquid Crystals with Positive Dielectric Anisotropy, Molecular Crystals and Liquid Crystals, 127:1, 389-395

To link to this article: http://dx.doi.org/10.1080/00268948508080853

Mol. Cryst. Liq. Cryst., 1985, Vol. 127, pp. 389–395
0026-8941/85/1274-0389/$15.00/0

Printed in the United States of America

Grain Boundaries Observation of Polycrystalline Silicon Using Nematic Liquid Crystals with Positive Dielectric Anisotropy†

TOSHIO TAKEUCHI and TADASHI TAKAHASHI

Department of Electronic Engineering, Sendai Radio Technical College,
Miyagicho Miyagi 989-31 Japan

and

TATSUO UCHIDA

Department of Electronic Engineering, Faculty of Engineering,
Tohoku University, Sendai 980 Japan

(*Received August 28, 1984*)

A new method to analyze electrically active grain boundaries of polycrystalline silicon by using a field effect of nematic liquid crystal with positive dielectric anisotropy is described. In addition, threshold voltage of a liquid crystal planar cell with interdigited comb metal electrodes is measured as a function of frequency and temperature. From the results, the fringing electric field effect on the liquid crystal molecular orientation is clarified. This method is advantageous in the wide frequency range ($0.1-10^5$ Hz), fast response time and low threshold voltage by comparison with the method using nematic liquid crystal with negative dielectric anisotropy.

Polycrystalline silicon films, ribbons and wafers are widely used in the field of silicon devices, such as interconnections of integrated circuits,[1] field effect transistors arrays[2] and solar cells.[3-5]

---

†Paper presented at The Tenth International Liquid Crystal Conference July 15–21, 1984, The University of York, UK.

Macroscopic electrical transport properties of these polycrystalline silicon has been extensively measured as a function of doping density and grain size. Resistivities, Hall mobilities, carrier concentrations of doped polycrystalline silicon has well understood with double depletion layers model.[6] But these models deal with grain boundaries as homogeneous potential barriers and measured experimental results show macroscopic transport properties of uniform materials without grain boundaries.

On the other hand, the knowledge of the individual macroscopic potential barrier profile of each grain boundaries are very important on the optoelectronic device applications, such as solar cells and photosensing devices. In these devices, grain boundaries are expected to have several deleterious effects, namely charge trapping in deep levels, recombination through deep levels, scattering induced mobility degradation.

The measurements of electrical potential barrier profile at the grain boundaries of polycrystalline silicon under bias voltage gives useful informations for better understanding of grain boundaries and development of their passivation methods.

The analysis method described in this paper represents improvements of a novel method originally described by Redfield.[7] In this technique, incident light to the liquid crystal cell is linearly polarized by a polarizer and reflected light is observed through the analyzer as shown schematically in Fig. 1. Polarized directions of the polarizer and analyzer are right-angled and the reflected light is observed by a microscope. The cell is constructed with a glass, 10 μm thick mylar

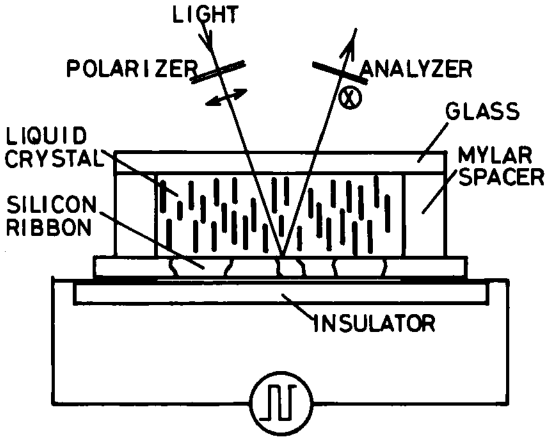

FIGURE 1 Experimental setup of test cell for grain boundaries observation.

film as a spacer and a polycrystalline silicon sample. Aluminum ohmic contacts are deposited on a square sample at two opposite edges. The surfaces of glass and silicon sample are treated with lecithin to align liquid crystal molecules perpendicular to the surfaces. As long as liquid crystal molecule align perpendicular to the surface, the polarized direction of incident light is not changed by the liquid crystal layer and therefore the reflected light cannot pass through the analyzer and dark state is observed. However, when a bias voltage is applied to the silicon sample, some grain boundaries induce potential drop higher than the other areas and fringing electric field into the liquid crystal changes the molecular orientation. The partially tilted molecular orientation causes the difference in the phase velocity of ordinally light and extraordinally light because of the refractive anisotropy of liquid crystal, by which the reflected light becomes elliptically polarized light and certain components of the light can pass through the analyzer and is observed as the bright portion.

In this method, Redfield has used a nematic liquid crystal with negative dielectric anisotropy (*n*-type nematic liquid crystal) and has reported the following results. (1) If a DC voltage is applied, patterns of grain boundaries extinguishes in a few seconds, so that the DC observation is not useful. (2) This cell does not respond to higher frequency. (3) 1-3 Hz is optimum frequency of applied voltage. (4) The effect is always observed near nematic isotropic phase transition temperature. Then we analyze the mechanism of orientation effects of Redfield's experimental results on *n*-type nematic liquid crystal cells.

Liquid crystals show dielectric anisotropy and conductivity anisotropy between the longitudinal (||) and perpendicular ($\perp$) to molecular axes. In Fig. 2 molecular orientation effects of *n*-type and *p*-type nematic liquid crystals are drawn schematically on both anisotropy under electric field. Using symbols $\epsilon_{\parallel}$, $\epsilon_{\perp}$ and $\sigma_{\parallel}$, $\sigma_{\perp}$ for dielectric constants and conductivities for parallel and perpendicular to the director respectively, *n*-type nematic liquid crystal anisotropy is expressed as follows,

$$\epsilon_{\parallel} < \epsilon_{\perp}, \qquad \sigma_{\parallel} > \sigma_{\perp} \tag{1}$$

Apparently from eq. (1), these anisotropies have different effect on the molecule orientation, that is, dielectric anisotropy has an effect to align the molecule perpendicular to the electric field and conductivity anisotropy parallel to it. For the higher frequency the ion current becomes undominant, so that orientation effect due to the conductivity anisotropy becomes negligible. On the other hand, for lower frequency conductivity anisotropy is effective and stronger effect

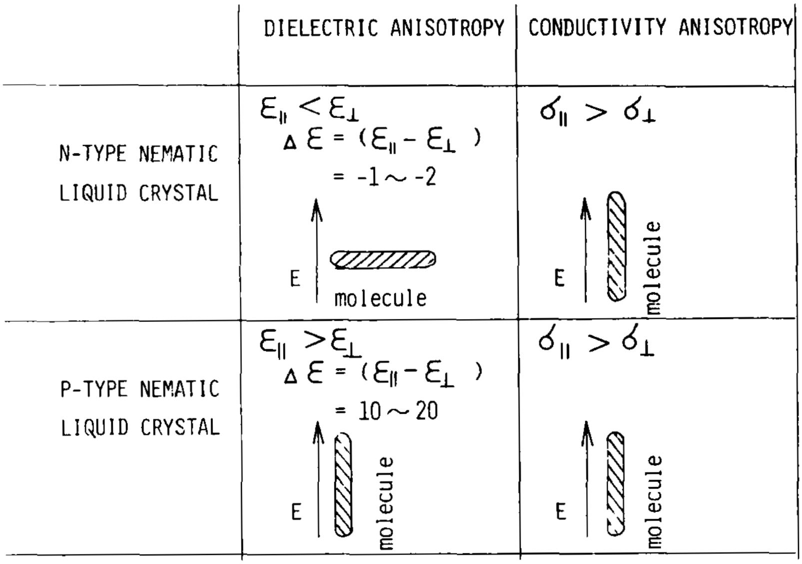

FIGURE 2 Schematic drawing of liquid crystal molecule under bias voltage for *n*-type and *p*-type nematic liquid crystals, also shows dielectric anisotropy and conductivity anisotropy.

between the conductivity anisotropy and dielectric anisotropy determines the orientation. This mechanism explains Redfield's results as follows: The fact that the field effects are not observed at high frequency is due to that the effect of ion current is undominant by comparison with the effect of dielectric anisotropy and orientational direction of the latter effect coincides with the original direction of molecular orientation. At lower frequency, orientation effect of the ion current and dielectric anisotropy compete with each other, and former becomes dominant at the higher temperature because ion current increases while dielectric anisotropy decreases according to temperature. In addition, the phenomenon that the orientation effects are observed at the instance of polarity change of the DC voltage is explained as the electric field attenuation by the charge up effects of ion current.

In our experiment to observe the grain boundaries, we used a nematic liquid crystal with positive dielectric anisotropy (*p*-type nematic liquid crystal) instead of the *n*-type nematic liquid crystals. The dielectric and conductivity anisotropies of *p*-type nematic liquid crystals are expressed as follows,

$$\epsilon_{\parallel} > \epsilon_{\perp}, \qquad \sigma_{\parallel} > \sigma_{\perp} \tag{2}$$

Schematic illustrations of anisotropies in *p*-type nematic liquid crystals both in dielectric and conductivity are shown in Fig. 2 comparing with *n*-type nematic liquid crystals. Apparently from eq. (2), both anisotropies are positive and have orientational effect to align liquid crystal molecules parallel to the electric field. Therefore, molecules align parallel to the substrate surface at the position of grain boundaries as shown in Fig. 3. The *p*-type nematic liquid crystals responds to the voltage from low frequency to high frequency because of the above mentioned mechanism.

To confirm the above discussions experimentally, a simulation cell with interdigited cobm metal electrodes deposited and photoeched on an insulating substrate instead of silicon plate is made, where the cobm electrodes is composed with aluminum with 3000 A thick, 34 μm width and 66 μm gaps. The surfaces of metal electrodes deposited substrate and cover glass were treated with lecithin to obtain the perpendicular alignment. Thin layer of *n*-type nematic liquid crystal material is mixture of 50 percent MBBA and 50 percent EBBA. Threshold voltage is optically measured by a microscope.

The measured threshold voltages are plotted in Fig. 4 as a function of its frequency, and parameter is substrate temperature. From the results shown in Fig. 4, the cell does not respond to higher frequency than 1–3 Hz and its threshold voltage decreases as the substrate temperature increases. These results fairly agree with Redfield's results and their mechanisms mentioned previously.

The experimental results for the same simulation cell with *p*-type nematic liquid crystal (GR-41 of Chisso Corp.) are shown in Fig. 5. Here the threshold voltage are plotted as a function of frequency. From Fig. 5, this cell responds in wide frequency range from 0.1 to 10^5 Hz and the threshold voltages are almost constant and independent of substrate temperature and frequency at the range of $10–10^4$

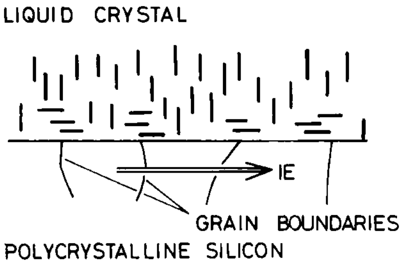

FIGURE 3 Horizontal alignment of the *p*-type nematic liquid crystal above the polycrystalline silicon by the fringing field from the grain boundaries, which shows high frequency response.

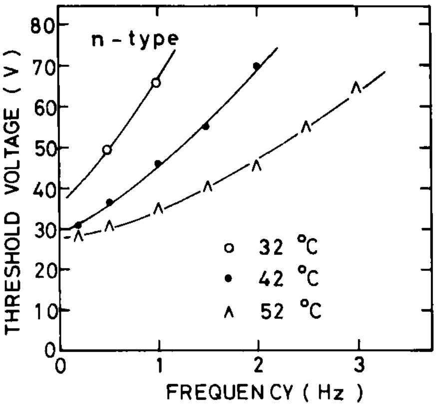

FIGURE 4 Threshold voltage vs frequency of *n*-type nematic liquid crystal modified cell. Parameter is cell temperature.

Hz where the effect of the dielectric anisotropy is considered to be dominant. In addition, the fact that the threshold voltage decreases according to decrease of frequency and increase of temperature for the lower frequency than 10 Hz is considered to be due to increase of the additional effect of ion current.

The application of *p*-type nematic liquid crystal to the observation of electrically active polycrystalline silicon grain boundaries is more effective than that of *n*-type nematic liquid crystal because the threshold voltage is low as well as it is independent of temperature and frequency at a certain range. Furthermore the brightness of the grain

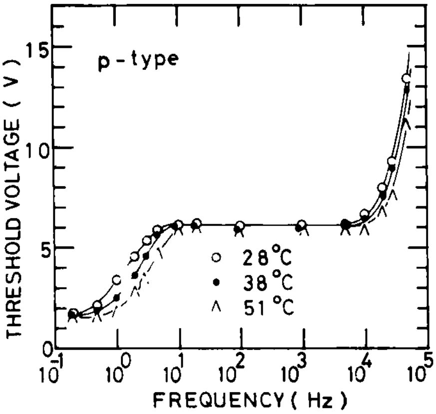

FIGURE 5 Threshold voltage vs frequency of *p*-type nematic liquid crystal modified cell. Parameter is cell temperature.

boundaries depends on electric field strength in the case of the *p*-type nematic liquid crystal, so that this method is useful for not only existence of the grain boundary but also for measuring the potential barrier height. This method using the *p*-type nematic liquid crystal is considered to be promising for analysis of rapid quenched polycrystalline silicon ribbons with small grain size.[4]

References

1. F. Faggin and T. Klein, *Solid-State Electron.* **13**, 1125 (1970).
2. Y. Hirai, Y. Osada, T. Komatsu, S. Omata, K. Aihara, and T. Nakagiri, *Appl. Phys. Lett.* **42**, 701 (1983).
3. T. F. Ciszek, G. H. Schwuttke, and K. H. Young, *J. Cryst. Growth* **46**, 527 (1979).
4. T. Takeuchi, K. I. Arai, and N. Tsuya, *J. Electron. Mater.* **9**, 111 (1979).
5. T. L. Chu, *Appl. Phys. Lett.* **29**, 675 (1976).
6. T. I. Kamins, *J. Appl. Phys.* **42**, 4357 (1971).
7. D. Redfield, *Appl. Phys. Lett.* **38**, 174 (1981).